



## Formulation and Evaluation of Voriconazole Loaded Nanosponges for Topical Delivery

Vijay Kumar Goli<sup>\*1</sup>, Maniraj nepali<sup>2</sup>, Amar Anand<sup>2</sup>, Y Sinduja<sup>2</sup>, N Uday Kiran<sup>2</sup>, Afzal emam<sup>2</sup>, Pravallika M<sup>2</sup>

<sup>1</sup>Department of Pharmaceutics, St. Mary's group of institution, Deshmukhi (Village), Pochampally (Mandal), Yadadri Bhuvanagiri (Dist), Telangana-508284, India

<sup>2</sup>St. Mary's group of institution, Deshmukhi (Village), Pochampally (Mandal), Yadadri Bhuvanagiri (Dist), Telangana-508284, India

### Article History:

Received on: 10 Jan 2023

Revised on: 25 Jan 2023

Accepted on: 27 Jan 2023

### Keywords:

Voriconazole,  
HP  $\beta$ -Cyclodextrin,  
Nanosponges,  
Drug Delivery System

### ABSTRACT

In this research, Voriconazole was first formed into a gel form, and then nanosponges were made using the solvent evaporation approach. By combining PVA into a co-polymer as well as HP-cyclodextrin and even HPMC K4M as rate-retarding polymers, the formulations for Nanosponges were produced. The compatibility of the medicine with formulation ingredients has been evaluated using Fourier Transform Infra-Red (FTIR) spectroscopy. We examined the surface morphology, yield, and drug entrapment effectiveness of the Nanosponges. SEM analysis was used to investigate the Nanosponges' shape and surface morphology. Nanosponges were discovered to be porous and spherical by scanning electron microscopy. SEM images showed that the Nanosponges were spherical in all configurations; however, at larger ratios, drug crystals were seen across the nanosponge surface. Improvement within the drug/polymer ratio (1:1 to 1:3), which takes place in ascending sequence due to the rise in polymer concentration, however after a certain level of concentration, it was noted that when the drug/polymer ratio rose, the particle size declined. All formulations' average particle sizes fall between 316.4 and 454.8 nanometers. The drug release of the optimised formulation was found to be 99.42%, while the drug content of other formulations ranged from 82.8 to 97.2% and their entrapment efficiencies from 86.24 to 96.88%. The optimised gel formulation's stability studies show that the formulated gel was stable up to 90 days.



1 \*Corresponding Author

2 Name: Vijay Kumar Goli

3 Phone: +91 9533344084

4 Email: gvijay304@gmail.com

6 eISSN: 2583-0953

7 DOI: <https://doi.org/10.26452/ijcpms.v3i1.455>



Production and Hosted by

Pharmasprings.com

© 2023 | All rights reserved.

### INTRODUCTION

In order to alter and regulate the releasing behaviour of the medications, there has been a lot of focus in recent years on the creation of innovative nanosponge base drug delivery systems [1]. It is possible to change the therapeutic index and duration of a drug's activity by incorporating the system into a carrier. The frequent inclusion of vitamins and -hydroxy acids in topical treatments, which have apparent and observable advantages - particularly in ageing or photodamaged skin - has encouraged consumers' growing interest in skin care and skin treatment products [2]. Despite being

23 very helpful, these substances can occasionally  
 24 cause irritation, which is often felt as burning,  
 25 stinging, or redness and is more common in people  
 26 having delicate skin. The formulators attempted  
 27 to address this issue using one of the two tech-  
 28 niques after realising the issue. They sacrificed  
 29 efficacy in order to lower the concentration of  
 30 these substances. Additionally, the vehicle has been  
 31 altered to improve the product's skin compatibility  
 32 or emolliency. Small, spherical, porous delivery  
 33 devices called nanosponges are made of porous  
 34 polymeric materials [3]. These are used to passively  
 35 target cosmetic compounds to the skin, which has  
 36 significant advantages like lowering the overall  
 37 dose, keeping the dosage form on the skin, as  
 38 well as preventing systemic absorption [4]. These  
 39 nanosponges can be successfully added to topical  
 40 systems for longer release as well as skin retention,  
 41 which lowers the variability in drug absorption,  
 42 toxicity, as well as improves compliance among  
 43 patients by extending dose intervals. Drug irritabil-  
 44 ity can be greatly reduced by nanosponges without  
 45 compromising their effectiveness. The diameter of  
 46 the nanosponge varies from 250 nm to 1  $\mu$ m [5].

## 47 METHODOLOGY

### 48 Pre-formulation studies:

49 Certain fundamental physical and chemical charac-  
 50 teristics of the drug molecule alone as well as cou-  
 51 pled with excipients must be established prior to the  
 52 construction of the nanosponge dosage form. Pre-  
 53 formulation is the name given to this initial learning  
 54 period. The pre-formulation process' main goal is to  
 55 produce data that will aid the formulator in creat-  
 56 ing stable, bioavailable dosage forms that might be  
 57 mass-produced [6].

58 The objectives of pre-formulation studies are:

59 To establish the drug substance's compatibility with  
 60 various excipients and to analytically assess the drug  
 61 substance and identify its necessary qualities.

### 62 Spectroscopic study:

#### 63 Identification of pure drug:

#### 64 Solubility studies:

65 Voriconazole's solubility was tested in a variety  
 66 of solvents, including distilled water, 0.1 N HCL,  
 67 buffers with a pH of 6.8, and organic solvents such  
 68 ethanol and methanol. Studies on drug solubility  
 69 involved putting an excessive amount of the drug in  
 70 various beakers with the solvents. The mixes were  
 71 shaken continuously for 24 hours. What man's filter  
 72 paper grade no. 41 was used to filter the solutions.  
 73 On the basis of spectrophotometry, the filtered solu-

tions were examined [7].

### Physicochemical parameters:

The substance was described as being a white to  
 off-white crystalline powder with no taste or odour,  
 according to descriptive language.

### Determination of absorption maximum ( $\lambda_{max}$ ):

The term "max" refers to the wavelength at which  
 light is absorbed the most. Every substance has this  
 "max," which is both characteristic of and helpful  
 in identifying the substance. It's crucial to deter-  
 mine the substance's maximum absorption rate for  
 precise analytical analysis. Since most medications  
 are aromatic or include double bonds, they absorb  
 radiation in the UV area (190-390 nm). 10mg  
 were weighed precisely. Separately, voriconazole  
 was dissolved in 10 ml of clean volumetric flask in  
 methanol. The same substance was diluted to a  
 volume of 10 ml to produce stock solution-I with  
 a concentration of 1000 g/ml. Pipette 1ml of the  
 stock solution I into a 10ml volumetric flask. Using  
 methanol buffer, the volume was increased to 10 ml  
 to generate stock solution II with a concentration  
 of 100 g/ml. 1 ml was pipette-out of stock solu-  
 tion II into a 10 ml volumetric flask. Using methanol  
 buffer, the volume was increased to 10 ml in order to  
 achieve a concentration of 10 g/ml. In order to reach  
 the absorption maximum (-max), A UV-visible dou-  
 ble beam spectrophotometer was then used to scan  
 this solution between 200 and 400 nm [8].

### Construction of calibration curve:

Voriconazole, accurately weighed at 10 mg, was dis-  
 solved in 10 ml of clean volumetric flask. A 6.8 ph  
 buffer was used to dilute the fluid to 10 ml, yielding  
 a concentration of 1000 g/ml. To get a concentra-  
 tion of 100 g/ml, 1 ml of this standard solution was  
 pipette out into a 10 ml volumetric flask and the vol-  
 ume was topped off with methanol. Aliquots of 0.2,  
 0.4, 0.6, 0.8, 1.0, and 1.2 ml from the aforementioned  
 stock solution were transferred to separate 10 ml  
 volumetric flasks, and the solution was diluted to 10  
 ml with methanol buffer to achieve concentrations  
 of 2, 4, 6, 8, 10, and 12 g/ml, respectively. At 247 nm,  
 the absorbance of each solution was determined [9].

### Drug excipient compatibility study:

Using Fourier Transform - Infra Red spectroscopy  
 (FT-IR), the compatibility of the medicine and excip-  
 ient was discovered. In order to ascertain whether  
 there might be any FT-IR spectra were obtained from  
 Bruker FT-IR Germany (Alpha T), and they were  
 used to study the relationships between the pure  
 drug and the excipients in the solid state. To make  
 potassium bromide pellets with a KBr press, the

127 solid powder sample has been crushed using a mortar  
128 with 100 times the quantity of potassium bromide.  
129 The powder was subsequently inserted into a stainless steel die as well as compressed between  
130 polished steel anvils at a pressure of around 8t/in<sup>2</sup>.  
131 The wavelengths of the spectra were between 4000  
132 and 400 cm<sup>-1</sup> [Table 1] [10].

### 134 Method of Preparation of Nanosponges:

135 By adopting the solvent evaporation process, nanosponges were created using various ratios  
136 of -cyclodextrin, HP -cyclodextrin, HPMC KM4 as a rate-retarder polymer, and co-polymers like  
137 polyvinyl alcohol. A specific amount of PVA in 100 ml of an aqueous continuous phase that had been  
138 created using a magnetic stirrer was slowly added to a disperse phase made up of Voriconazole (1 gm)  
139 and the necessary amount of PVA dissolved in 10 ml of solvent (ethanol). On a magnetic stirrer, the  
140 reaction mixture was agitated at 1000 rpm for three hours. The created nanosponges were collected by  
141 filtering them through Whatman filter paper and allowed to dry for two hours at 50°C in the oven.  
142 In order to guarantee that any remaining solvent was removed, the dried nanosponges were kept in  
143 vacuum desiccators [11].

### 152 Evaluation parameters of Nanosponges:

153 The Nanosponges was evaluated for various parameters:-

154 Entrapment efficiency

155 Scanning electron microscopy

156 Particles size and shape

### 158 Entrapment efficiency

159 The 100mg Voriconazole weight equivalent nanosponge was dissolved in 10ml of distilled  
160 water for analysis. Ten millilitres of the transparent layer of the medication after it has been dissolved is  
161 taken.

162 After that, a UV spectrophotometric technique at 247 nm (U.V Spectrophotometer, Systronics)  
163 was used to determine how much medication was present in the water phase. With a different  
164 nanoparticulate sample, the experiment was repeated.

165 The concentration of the medication in the clear supernatant layer was determined using the UV-  
166 spectrophotometric technique after centrifuging the suspension at 500 rpm for five minutes. The calibration  
167 curve is used to determine the drug's concentration [12].

168 By deducting the quantity of drug in the nanoparticle suspension divided by the amount of drug in the

178 aqueous phase, a percentage of drug inside the particles was estimated. The following equation was  
179 used to calculate the drug's entrapment efficiency (%) .

$$\begin{aligned} & \% \text{ of Drug entrapment} = \\ & \left( \frac{\text{Mass of drug in nanosponge}}{\text{Mass of drug used in formulation}} \right) \\ & \times 100 \end{aligned}$$

### 183 Scanning electron microscopy

184 Scanning electron microscopy is used to examine the morphological characteristics of prepared  
185 nanosponges at various magnifications.

### 187 Particle size and shape

188 Malvern Zetasizer ZS was used to measure the average particle size and shape of the synthesised  
189 nanosponges utilising water as the dispersions medium [13]. To determine the size of the particles,  
190 the sample were scanned [Figure 1].

### 193 Formulation of Nanosponge loaded gel:

194 To achieve smooth dispersion, the polymer was first agitated at 600 rpm for two hours while  
195 being soaked in water for the gel for two hours. To balance the pH, triethanolamine (2% v/v) was  
196 added. Thus, the previously manufactured, optimised nanosponge was added, and the aqueous  
197 dispersion was given an ethanolic solution of the permeation enhancer, propylene glycol [Table 2].  
198 Table 4 displays the composition of nanosponge gels [14].

### 204 Visual Appearance and Clarity:-

205 Under fluorescent lighting, on a white and black background, visual appearance and clarity were  
206 checked for the presence of any particle matter [15].

### 209 pH:

210 After all the materials had been added, a pH metre was used to determine the pH of the created in-situ  
211 gelling system [16].

### 213 Drug Content uniformity:

214 Utilising a spectrophotometric technique, drug content homogeneity of generated in-situ gelling systems  
215 was assessed.

216 Pipetting 1 ml of each optimised formulation and diluting it up to 100 ml with Simulated Tear Fluid  
217 (pH 6.8) was used to assay these formulations. The mixtures were agitated for two to three minutes  
218 until a clear gel solution was obtained.

219 The solution was filtered using Millipore membrane filtrate (0.45um), and a UV-Visible spectrophotometer  
220 was used to detect the absorbance at 247 nm [17].

**In-Vitro Gelation:-**

The ability of formulations containing various ratios of poloxamer and HPMC to gel was assessed. It was carried out by adding a drop of polymeric solution to vials containing 1 ml of freshly made and equilibrated Simulated Tear Fluid and visually timing how long it took for the gel to form and disintegrate [18].

**Rheological Studies:-**

By taking into account the formulation's viscosity, it is crucial to calculate the drug's residence duration in the eye. At physiological temperature, the prepared solutions were allowed to gel before the viscosity was measured using a Brookfield viscometer (Brookfield DV+Pro, Brookfield Engineering Laboratories, Middleboro, MA, USA).

**In vitro Drug Release studies of nanosponge gel formulations:**

Using the dialysis membrane method, in vitro assessment experiments of topical gel were carried out. The membrane was submerged in 0.1N HCl for 12 hours, then 6.8pH phosphate buffer was added to the receptor compartment. A test substance equal to 100mg was equally placed to the membrane's surface. To prevent air bubbles from getting trapped under the prepared membrane, the cell was carefully mounted with the membrane in place. The entire assembly was kept at 37°C for 12 hours while stirring was done at a continuous 600 rpm. At 1-hour intervals, aliquots of the drug sample (4 mL) were obtained and replaced with an equal volume of freshly made buffer [63]. Three duplicates of each experiment were carried out. The UV spectrophotometer was used to analyse the drugs at 247 nm [19].

**Modelling of Dissolution Profile:**

To explain the release kinetics of voriconazole from the matrix tablets in the current investigation, data from the in vitro release were fitted to several equations and kinetic models.

The kinetic models employed were the Higuchi release, Zero Order Equation, First Order, and Korsmeyer-Peppas models.

Kinetic Research: Models in mathematics:

To interpret the release rate of the drug from matrix systems for the optimised formulation, various release kinetic equations (zero-order, first-order, Higuchi's equation, and Korsmeyer-Peppas equation) were used [20].

Calculated was the best match with the highest correlation (r<sup>2</sup>).

**Zero-order model:**

The equation can be used to illustrate medicine absorption from dose forms that gradually release the medication but do not break down.

$$Q_t = Q_0 + K_0t$$

**First Order Model:**

In general, release behaviour follows the first order equation below:

$$\log C = \log C_0 - kt/2.303$$

**Higuchi model:**

The Higuchi model is generally stated by the following equation.

$$Q = K_H \cdot t^{1/2}$$

Where,  $K_H$  is the Higuchi dissolution constant.

**Korsmeyer-Peppas model**

First, to determine the mechanism of drug release, 60% of the drug release data were fitted into the Korsmeyer-Peppas model.

$$M_t / M_\infty = Kt^n$$

Only the part of the release curve where  $M_t / M_0.6$  should be considered to determine the exponent of n.

Log cumulative percentage drug release vs log time was used to illustrate data from in vitro drug release investigations to analyse the release kinetics [Table 3].

**Stability studies:**

In order to ascertain the physical and chemical stabilities, the optimised formulation was stored for stability testing for a period of three months at ambient (30 °C), refrigerator (4 °C), as well as accelerated (40 °C, 75%RH) conditions.

The formulation was assessed aesthetically, for drug release after 30, 60, and 90 days, and for entrapment effectiveness.

**RESULTS AND DISCUSSIONS****Voriconazole Characterization:****Physical Properties:**

Studying the physicochemical characteristics of the bulk drug is important in order to manufacture the medicinal ingredient into a dosage form.

A. Colour: white colour

B. Melting Point: 129-134°C

C. Solubility: Solubility of Voriconazole was conducted using various solvents, including distilled water, 0.1N HCL, as well as 6.8 pH buffers.

**Table 1: Formulation table of Voriconazole loaded nanosponges**

S.NO	Excipients	F1	F2	F3	F4	F5	F6
1	Voriconazole (gm)	0.5	0.5	0.5	0.5	0.5	0.5
2	PVA (gm)	0.5	0.5	0.5	0.5	0.5	0.5
3	HPMC K 4M (gm)	0.5	1.0	1.5	-	-	-
4	HP $\beta$ cyclodextrin	-	-	-	0.5	1.0	1.5
5	Ethanol (ml)	10	10	10	10	10	10
6	Water	100	100	100	100	100	100

**Table 2: Formulation of Nanosponge loaded gel**

Ingredients	F7	F8	F9
Optimize Nanosponge(mg)	400	400	400
Xanthan gum	100		
Guar gum		100	
Karaya gum			100
Propylene Glycol(ml)	1	1	1
Distilled Water(ml)	5	5	5
Triethanolamine(2%v/v)(ml)	1	1	1

**Table 3: Drug transport mechanisms suggested based on 'n' value**

S. No	Release exponent	Drug transport mechanism	Rate as a function of time
1	0.5	Fickian diffusion	$t^{-0.5}$
2	$0.45 < n = 0.89$	Non -Fickian transport	$t^{n-1}$
3	0.89	Case II transport	Zero order release
4	Higher than 0.89	Super case II transport	$t^{n-1}$

**Table 4: Solubility of Voriconazole**

S.No	Buffer	Solubility (mg/ml)
01	Water	0.224
02	Ethanol	1.42
03	Methanol	0.926
04	0.1 N HCL	0.458
05	6.8 pH buffer	3.678

**Table 5: Calibration curve data of Voriconazole**

Concentration	Absorbance
0	0
2	0.154
4	0.311
6	0.472
8	0.628
10	0.792
12	0.956

**Table 6: Particle size of Nanosponges**

S.NO	Formulation code	Particle size (nm)
1	F1	321.6
2	F2	398.2
3	F3	218.2
4	F4	396.4
5	F5	454.8
6	F6	416.4

**Table 7: Drug content of Formulated Nanosponges**

Formulation code	Mean % drug content
F1	88.22
F2	94.60
F3	97.12
F4	92.64
F5	97.08
F6	90.82

**Table 8: Entrapment efficiency of Nanosponges**

Formulation code	Entrapment efficiency %
F1	90.86
F2	95.12
F3	96.54
F4	92.84
F5	95.88
F6	90.12

**Table 9: Visual appearance and clarity of all (F7-F9) formulations**

Formula	Appearance	Clarity
F7	Transparent	Clear
F8	Transparent	Clear
F9	Transparent	Clear

**Table 10: pH measurements of all formulations (F7-F9)**

Formula	pH
F7	6.6
F8	6.8
F9	6.9

**Table 11: Drug content of Formulated gels**

Formulation Code	Drug content
F7	95.52 ± 0.47
F8	96.31 ± 0.56
F9	98.15 ± 0.69

**Table 12: Gelling capacity of all formulations (F7-F9)**

Formulation	Gelling capacity at 25 °C	Gelling capacity at 37°C
F7	—	+
F8	---	++
F9	—	+++

+ Gelation dissipates quickly after 50–60 seconds; ++ Gelation occurs in 60 seconds and is stable for 3 hours; +++ Gelation occurs in 60 seconds and lasts for 6 hours

**Table 13: Viscosity Studies of Formulations**

Angular Velocity (rpm)	F7	F8	F9
10	103.0	107.1	112.3
100	96.0	97.4	99.2

**Table 14: In vitro diffusion studies of Voriconazole Nanospongein corporated gel**

Time (hrs)	F7	F8	F9
0	0	0	0
1	15.42	12.46	9.12
2	27.29	23.48	12.71
3	46.62	34.28	26.63
4	53.04	42.12	38.12
5	60.78	50.16	44.68
6	71.82	58.06	50.54
7	77.94	67.82	62.24
8	85.92	79.68	73.26
9	92.96	87.24	78.12
10	98.12	96.12	83.36
11		99.56	89.90
12			94.14

**Table 15: Regression Values**

S.NO	Zero order	First order	Higuchi	Peppas
Code	R <sup>2</sup>	R <sup>2</sup>	R <sup>2</sup>	R <sup>2</sup>
F9	0.988	0.929	0.935	0.844

**Table 16: Gelling capacity of all formulations (F9)**

Formulation	Gelling capacity at 25 °C	Gelling capacity at 37°C
30th day	+++	+++
60th day	+++	+++
90th day	+++	+++

**Table 17: Drug content of Formulated gels**

Formulation Code	Drug content
30th day	98.05 ± 0.54
60th day	97.98 ± 0.11
90th day	97.85 ± 0.64



**Figure 1: Photography representation of Malvern zeta sizer used for finding particle size & zeta analysis**

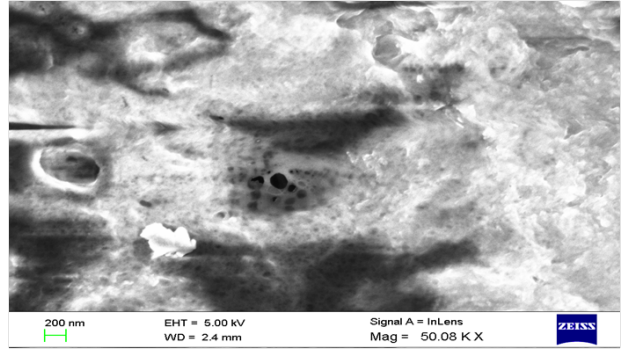


**Figure 6: Nanosponges structure optimized formulation (F3)**

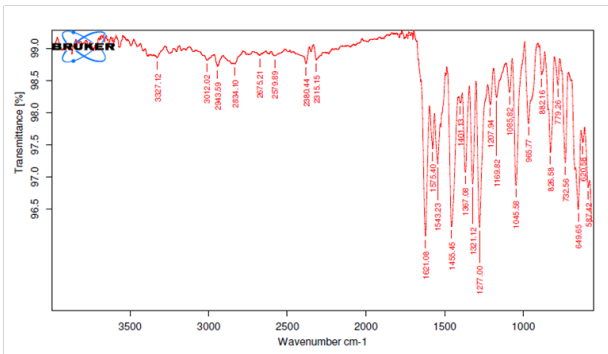


**Figure 2: FTIR Spectra of Pure Drug**

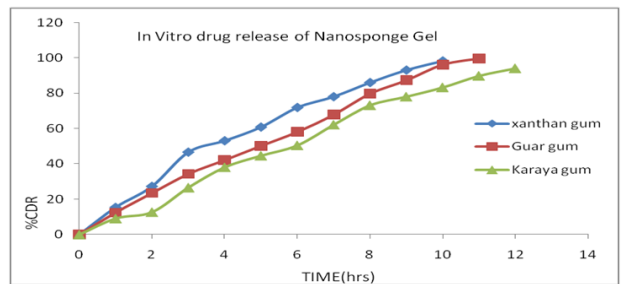


**Figure 7: Percentage of drug release graph F7-F9**

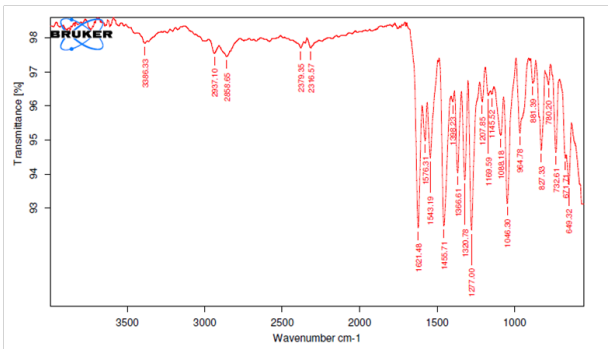


**Figure 3: FTIR Spectra of drug and excipients**

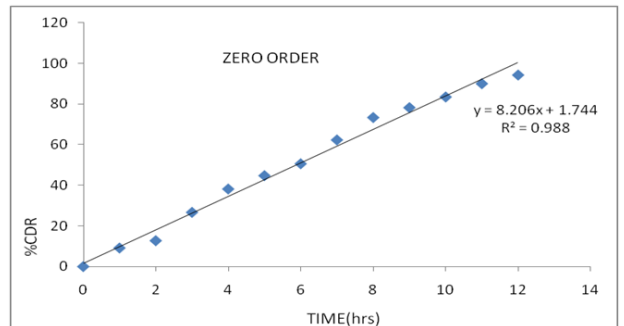


**Figure 8: Zero Order Plot for F9**

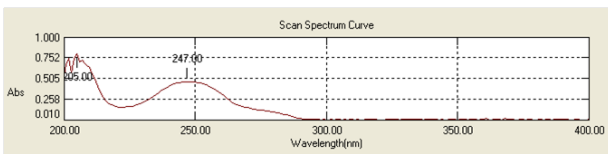


**Figure 4: λ-max in 6.8 phosphate buffer**

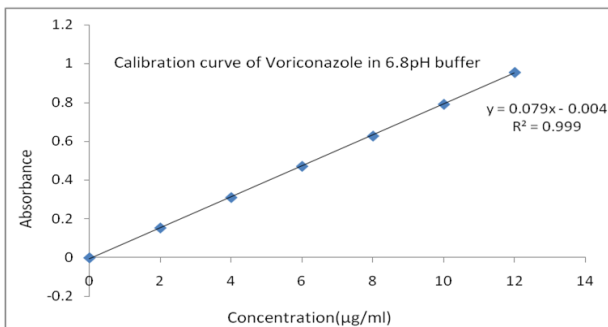


**Figure 5: Calibration Curve of Voriconazole in 6.8 pH phosphate buffer**

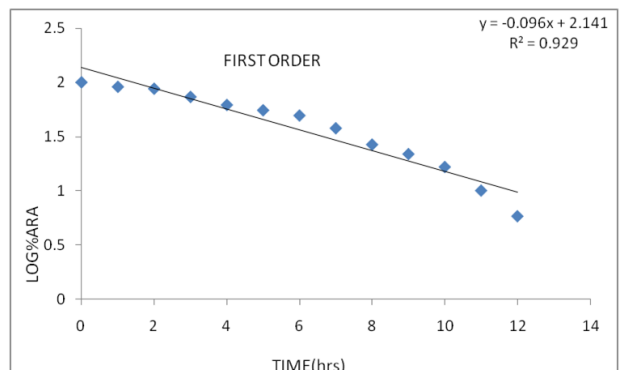


**Figure 9: First Order Plot for F9**



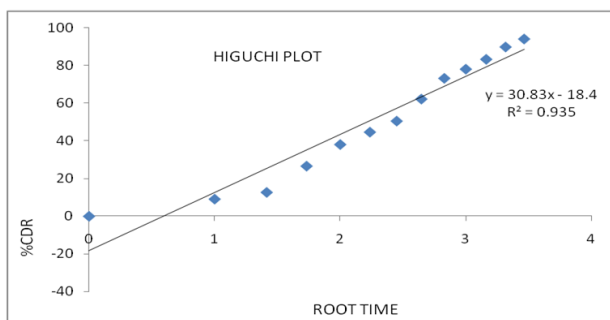


Figure 10: Higuchi Plot for F9

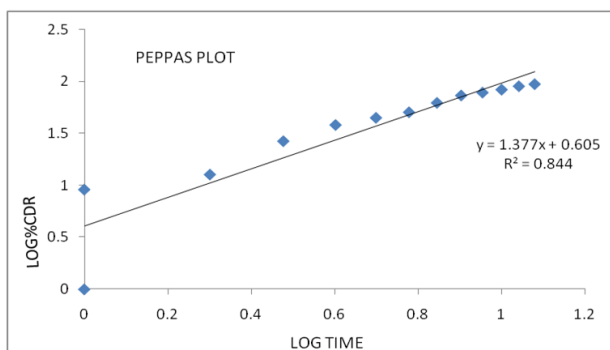


Figure 11: Peppas Plot for F9

### Discussion

According to the aforementioned solubility studies, 6.8 pH phosphate buffer has a higher solubility of the medication than the other buffers. More ethanol than methanol was found to be solubilized in organic solvents.

### Drug excipient compatibility:

By comparing the spectra of the FT-IR analysis of the pure drug with those of the various excipients employed in the formulation, the compatibility of the drug and excipient was established [Figures 2 and 3].

### Discussion:

#### Spectral data:

The major functional groups are primary amine, nitro, and carbonyl group

Obtained peak in IR spectra are as follows.

#### IR (KBr) $\text{cm}^{-1}$ :

732.50-732.61(CH- bending), 1169 (C=C stretching), 1277 (C-O stretch in aromatic compound), 1456 (C-C "oop" in aromatic compound) 1543 (N-N stretching).The spectral data confirm the structure of the compound.

### Discussion

It indicates that the excipients employed in the formulation were compatible with the medicine because it was intact and had not interacted with

them. The medication is therefore in a free condition and can readily release from the polymeric network in its free form.

### Determination of absorption maximum ( $\lambda_{\text{max}}$ )

For a precise quantitative evaluation of the drug dissolution rate, the Voriconazole $\lambda_{\text{max}}$  was determined in a 6.8 pH phosphate buffer [Figure 4].

### Discussion

As indicated in [Figure 4] the maximum absorbance of voriconazole in pH 6.8 buffer was discovered to be 247 nm.

Therefore, 247nm was chosen as the wavelength for the drug analysis in the dissolution media.

### Calibration curve

In 6.8 phosphate buffer, a linearity of 2–12 g/ml was discovered. As the regression value approached 1, it became clear that the procedure followed Beer-Lambert's law [Table 5 , Figure 5].

### Particle size analysis of Nanosponges:

By using optical microscopy to measure the nanosponges' particle sizes, it was discovered that their sizes were uniform. The average particle size of all formulations ranged from 316.4 nm to 454.8 nm and increases with increasing polymer concentration, however It was discovered that as the ratio of medication to polymer increased after a certain concentration, the particle size decreased. This may be because there was substantially less polymer available per nanosponge when the medication to polymer ratio was high. High drug-polymer ratios likely result in less polymer being present around the drug, a thinner polymer wall, and smaller nanosponges. The results of the particle size analysis show that The ratio of the polymer to medication concentration affects the formulation's particle size [Table 6].

### Morphology determination by scanning electron microscopy (SEM):

The morphology of the produced nanosponges utilising scanning electron microscopy (SEM), was investigated. SEM may be used to determine the shape and dimensions of microscopic specimens with particles that are as tiny as 10 to 12 grams. An electron beam scanned the sample in a predetermined pattern inside a chamber that had been evacuated.

A multitude of When the electron beam interacts with the object, physical phenomena result and when they are noticed, they are utilised to create images and reveal fundamental details regarding the specimens. The nanosponges were seen to be homo-

401 geneous, spherical, and free of any drug crystals on  
402 the surface.

403 The size of spherical nanosponges in terms of sur-  
404 face area and surface area per unit weight are influ-  
405 enced by the shape of the nanosponges.

406 The dissolution rate that exists in the dissolution  
407 environment may be impacted by the irregular  
408 shape of the particles [Figure 6].

#### 409 Drug content

410 The drug content ranged from 82.8 to 97.2% for the  
411 Nanosponges (F1-F6) that were developed [Table 7  
412 ].

#### 413 Discussion:

414 Formulation F1 had an 88.2% drug content, Formu-  
415 lation F2 had a 94.60% drug content, Formulation  
416 F3 had a 97.12% drug content, Formulation F4 had a  
417 92.64% drug content, Formulation F5 had a 97.08%  
418 drug content, and Formulation F6 had a 90.82%  
419 drug content.

#### 420 Entrapment efficiency:

421 It is computed to determine the effectiveness of any  
422 process, which aids in choosing the best method of  
423 production.

424 Following formulation preparation, the Practical  
425 Yield was determined by comparing the amount of  
426 Nanosponges recovered from each preparation to  
427 the total starting material (Theoretical yield).

428 It can be computed using the formula below [Table 8  
429 ].

$$430 \frac{\text{Entrapment efficiency}}{(\text{Practical yield}/\text{Theoretical yield (drug + polymer)}) \times 100} =$$

#### 433 Discussion

434 The entrapment efficiency of formulation F1 was  
435 found to be 90.86%, that of formulation F2 to be  
436 95.12%, that of formulation F3 to be 96.54%, that  
437 of formulation F4 to be 92.84%, that of formulation  
438 F5 to be 95.88%, and that of formulation F6 to be  
439 90.12%. F3 exhibits a high entrapment efficiency of  
440 96.54% among all the formulations.

#### 441 Visual Appearance and Clarity:

442 All of the formulations (F7-F9) were clear and trans-  
443 parent in appearance, and both at room tempera-  
444 ture and when refrigerated, the formulations were  
445 liquid [Table 9].

#### 446 pH Measurement

447 The formulations all have appropriate pH values  
448 between 6.6 and 6.9, which is suitable for ocular  
449 administration [Table 10].

#### Drug Content Uniformity

450 The prepared gels' medication content was discov-  
451 ered to be adequate, ranging from 95.52 to 98.15 %  
452 [Table 11].

#### Gelling Capacity

453 When tested, every composition displayed immedi-  
454 ate gelation contact with buffer. However the nature  
455 of the gel formed depended on the concentration of  
456 the polymer used [Table 12].

#### 459 Rheological Studies: -

460 A Brookfield DV 3 The viscosity of the sample was  
461 assessed using a programmable rheometer, formu-  
462 lations by changing the angular velocities or the  
463 shear rate. Formulations F7 through F9 had viscosi-  
464 ties that ranged from 96.0 to 112.3 cps at 100 rpm.  
465 Viscosity dropped as the rotational velocity rose,  
466 showing no thixotropic characteristic [Table 13].

#### 467 Discussion

468 The nanosponge formulation containing Karaya  
469 gum released the most amount of the drug, but  
470 xanthan gum and guar gum did not exhibit sus-  
471 tained drug release, according to the aforemen-  
472 tioned invitro experiments. The karaya gum-  
473 containing formulation F9 was therefore regarded  
474 as the ideal formulation. For the F9 formulation,  
475 drug release kinetics were carried out [Table 14, Fig-  
476 ure 7].

#### 477 Regression values of F9

478 For Zero order, First order, Higuchi, and Korsmeyer  
479 Peppas, the optimised formulation F9 has coeffi-  
480 cient of determination (R<sup>2</sup>) values of 0.988, 0.929,  
481 0.935, and 0.844, respectively. Data was fitted  
482 into the Korsmeyer Peppas equation, which demon-  
483 strated linearity with the Higuchi plot's regression  
484 line slope, which reflects the rate of drug release  
485 through the mode of diffusion, the n value of 1.377  
486 for an optimised formulation, to further confirm the  
487 diffusion mechanism. Thus, the Super case trans-  
488 port mechanism is indicated by the n number. As  
489 a result, the Higuchi model provided the greatest fit  
490 for the release kinetics of the optimised formulation,  
491 which demonstrated zero order drug release with  
492 a super case transport mechanism [Figures 8, 9, 10  
493 and 11 and Tables 15 and 16].

#### 494 Drug Content Uniformity:

495 According to stability experiments of Nanosponges  
496 loaded gel utilising karaya gum, the drug concentra-  
497 tion and gelling capacities were determined to be  
498 satisfactory because there was little change in either  
499 at the time of formulation or 90 days later [Table 17  
500 ].

## 501 CONCLUSION

502 The optimized formulation F9 has good gelling  
503 property with pH of 6.9, and drug content of 98.15%  
504 and coefficient of determination (R<sup>2</sup>) values for  
505 zero order, first order, Higuchi, and Korsmeyer pep-  
506 pas of 0.970, 0.731, 0.966, and 0.768, respectively.  
507 Data was fitted into the Korsmeyer Peppas equa-  
508 tion, which demonstrated linearity with the Higuchi  
509 plot's regression line's slope, which represents the  
510 rate of drug release through the mode of diffusion,  
511 the n value of 1.377 for an optimised formulation,  
512 to further confirm the diffusion mechanism. Thus,  
513 the super case transport method is indicated by the  
514 n value. As a result, the Higuchi model provided  
515 the greatest fit for the release kinetics of the opti-  
516 mised formulation, which demonstrated zero order  
517 drug release with a super case II transport mecha-  
518 nism. The stability studies revealed that the formu-  
519 lated Nanosponge gel uncovered to be stable for the  
520 period of 90days.

## 521 ACKNOWLEDGEMENT

522 I would like to thank Principal sir (Dr.V. Goutham) St.  
523 Mary's Group of Institutions, Deshmukhi (Village),  
524 Pochampally (Mandal), Yadadri Bhuvanagiri (Dist),  
525 Telangana-508284, India.

## 526 Conflict of Interest

527 The authors attest that they have no conflict of inter-  
528 est in this study.

## 529 Funding

530 No Funding.

## 531 REFERENCES

- 532 [1] R Sharma, B Roderick, and K Pathak. Evalua-  
533 tion of kinetics and mechanism of drug release  
534 from Econazole nitrate Nanosponges loaded  
535 carbopol Hydrogel". *Indian J of Pharma Edu and*  
536 *research*, 45(1):25–31, 2011.
- 537 [2] Z Rana, Patil Gunjan, and Z Zahid. Nanosponge  
538 - a completely new nano- horizon: pharmaceu-  
539 tical applications and recent advances. *Drug*  
540 *Dev Ind Pharm*, 2012.
- 541 [3] F David. Nanosponge drug delivery system  
542 more effective than direct injection. 2010.  
543 Physorg.com.
- 544 [4] S Zuruzi, N C Macdonald, M Moskovits, and  
545 A Kolmakov. Metal oxide nanosponges as  
546 chemical sensors: Highly sensitive detec-  
547 tion of hydrogen using nanosponge titania".  
548 *Angewandte Chemie International Edition*,  
549 46(23):4298–4301, 2007.
- [5] S Nacht and M Kantz. The Microsponge: A  
550 Novel Topical Programmable Delivery System,  
551 In: *Topical Drug Delivery Systems*", David WO,  
552 Anfon H A editors. *Marcel Dekker*, 42:299–325,  
553 1992. 554
- [6] M Kilicarslan and T Baykara. The effect of the  
555 drug/polymer ratio on the properties of Vera-  
556 pamil HCl loaded microspheres. *Int J Pharm*,  
557 252:99–109, 2003. 558
- [7] M Madhuri Reddy, Gundala Deepika, Meesala  
559 Simon, and Pothireddy Bharat. Golam Sofi-  
560 ullah SK, & Addakula Varalaxmi. Formulation  
561 and Evaluation of Nitrofurantoin Microspheres  
562 Loaded in Hard Gelatin Capsule. *Interna-*  
563 *tional Journal of Experimental and Biomedical*  
564 *Research*, 1(1):23–29, 2022. 565
- [8] K A Ansari, P R Vavia, F Trotta, and R Cavalli.  
566 Cyclodextrin-based nanosponges for delivery  
567 of resveratrol: in vitro characterisation, stabil-  
568 ity, cytotoxicity and permeation study. *AAPS*  
569 *PharmSciTech*, 12(1):279–86, 2011. 570
- [9] Y Ramesh, B Sarayu, Hari Chandana, G Nee-  
571 lima, and O Sana. Formulation and Evalua-  
572 tion of Lamivudine Nanosuspension. *Journal*  
573 *of Drug Delivery and Therapeutics*, 11(4-S):71–  
574 77, 2021. 575
- [10] F C Carvalho, M L Bruschi, R C Evangelista, and  
576 Mpd Gremio. Mucoadhesive drug delivery sys-  
577 tem. *Brazilian Journal of Pharmaceutical Sci-*  
578 *ences*, 46(1):1–17, 2010. 579
- [11] K P Meena, J S Dang, P K Samal, and K P  
580 Namedo. Recent advances in microsphere  
581 manufacturing technology. *International Jour-*  
582 *nal of Pharmacy and Technology*, 3(1):854–  
583 855, 2011. 584
- [12] K Krishnamoorthy and M Rajappan.  
585 Nanosponges: A novel class of drug deliv-  
586 ery system review. *J Pharm Pharm Sci*,  
587 15(1):103–114, 2012. 588
- [13] S Selvamuthukumar, S Anandam, K Kannan,  
589 and R Manavalan. Nanosponges: A Novel Class  
590 of Drug Delivery System- Review. *JPharm Phar-*  
591 *maceut Sci*, 15(1):103–111, 2012. 592
- [14] Nileshj, J Ruchi, T Navneet, Brham Prakash,  
593 and G Deepak Kumar. Nanotechnology :  
594 A Safe and Effective Drug Delivery Systems.  
595 *Asian Journal of Pharmaceutical and Clinical*  
596 *Research*, pages 159–165, 2010. 597
- [15] G Utzeri, P M Matias, D Murtinho, and A J  
598 Valente. Cyclodextrin-Based Nanosponges:  
599 Overview and Opportunities. *Frontiers in*  
600 *Chemistry*, 10, 2022. 601
- [16] J A Girigoswami, A Girigoswami, and K. Ver-  
602

- 603 satile Applications of Nanosponges in Biomed-  
604 ical Field: A Glimpse on SARS-CoV-2 Man-  
605 agement. *Bionanoscience*, 12(3):1018–1031,  
606 2022.
- 607 [17] K Tiwari and S Bhattacharya. The ascension of  
608 nanosponges as a drug delivery carrier: prepa-  
609 ration, characterization, and applications. *J*  
610 *Mater Sci Mater Med*, 4(3):28–28, 2022.
- 611 [18] R Lala and C Gargote. Current trends in  $\beta$ -  
612 cyclodextrin based drug delivery systems. *Int J*  
613 *Res Ayur Pharm*, 2(5):1520–1526, 2011.
- 614 [19] Jenny A Merima, P Alberto, and F Francesco.  
615 Role of  $\beta$ - cyclodextrin nanosponges in  
616 polypropylene photooxidation. *Carbohydrate*  
617 *Polymers*, 86:127–135, 2011.
- 618 [20] S Shankar, P Linda, S Loredana, T Francesco,  
619 V Pradeep, A Dino, T Michele, Z Gianpaolo, and  
620 C Roberta. Cyclodextrin based nanosponges  
621 encapsulating camptothecin: Physicochemical  
622 characterization, stability and cytotoxicity. *Eur*  
623 *J Pharm Biopharm*, 74:193–201, 2010.

**Copyright:** This is an open access article distributed under the terms of the Creative Commons Attribution-NonCommercial-ShareAlike 4.0 License, which allows others to remix, tweak, and build upon the work non-commercially, as long as the author is credited and the new creations are licensed under the identical terms.

**Cite this article:** Vijay Kumar Goli, Maniraj nepali, Amar Anand, Y Sinduja, N Uday Kiran, Afzal emam, Pravallika M. **Formulation and Evaluation of Voriconazole Loaded Nanosponges for Topical Delivery.** Int. J. of Clin. Pharm. Med. Sci. 2023; 3(1): 10-21.



624

625 © 2023 Pharma Springs Publication.